Nanoscale Research Letters
a SpringerOpen Journal

NANO EXPRESS   **Open Access**

CrossMark

Surfactant-Assisted Hydrothermal Synthesis of PMN-PT Nanorods

Chuan Li[1], Xingzhao Liu[1*], Wenbo Luo[1], Dong Xu[1,2] and Kai He[2]

Abstract

The effects of surfactant polyacrylate acid (PAA) on shape evolution of $0.7Pb(Mg_{1/3}Nb_{2/3})O_3$-$0.3PbTiO_3$ (0.7PMN-0.3PT) nanorods were studied. The results revealed that the polyacrylic acid content had great influence on the morphology of 0.7PMN-0.3PT. With increasing PAA concentration from 0.45 to 0.82 g/ml, the ratio of perovskite phase (PMN-PT nanorod) increased, while the ratio of pyrochlore phase decreased. When the PAA concentration was 0.82 g/ml, pure 0.7PMN-0.3PT nanorods were obtained. However, when PAA concentration was higher than 0.82 g/ml, the excess of PAA would hindered their [100] orientation growth. The piezoelectric coefficient d_{33} of 0.7PMN-0.3PT nanorod was obtained by linear fitting, and the d_{33} value was 409 pm/V.

Keywords: 0.7PMN-0.3PT, Nanorods, Piezoelectric materials, Hydrothermal, Microstructure

Background

Perovskite-typed ferroelectric materials have relatively high piezoelectric constant, such as $(1-x)PbZn_{1/3}Nb_{2/3}O_3$-$xPbTiO_3$ (PZNT) [1], Pb-based lanthanum-doped zirconate titanates (PZT) [2], and $BaTiO_3$ [3], which have been widely applied in the self-powered sensors [4–6] and energy conversion devices [7, 8]. Some non-ferroelectric lead-free materials also have good piezoelectric properties, such as ZnO [9] nanorod-based nanogenerator could provide an output voltage of 2 V, which has been demonstrated to drive a small light-emitting diode (LED) [10]. However, the actual publication may need more powerful piezoelectric material to make nanodevices.

Compared with other piezoelectric materials, a solid solution $(1-x)Pb(Mg_{1/3}Nb_{2/3})O_3$-$xPbTiO_3$ (PMN-PT) compound is promising for both further research and applications due to its high piezoelectric effect of 2500 pm/V [11–13]. Sun et al. [14] indicated that the nanorod of PMN-PT are good candidates than bulks in mechanical energy harvesting due to their high strain tolerance and the larger output power generated by PMN-PT. The piezoelectric properties of the PMN-PT ceramics may have been studied, but the PMN-PT nanorod rarely has been studied systematically. Xu

et al. [15] firstly synthesized the 0.72PMN-0.28PT nanorod via hydrothermal method; it has a piezoelectric constant 15 times higher than ZnO nanowire and 3 times higher than PZT nanowire.

Hydrothermal method is a versatile method to synthesize ceramic nanoparticles and nanowires. The hydrothermal reaction is a complicated progress; a tiny vary in the synthesis progress would change the final morphology of the product. In this letter, we investigated the influences of the surface active agent on the synthesis progress of the PMN-PT nanorods. It is found that the polyacrylic acid content could have great influence on morphology of the PMN-PT nanorods. The piezoelectric coefficient of 0.7PMN-0.3PT nanorod has also been tested.

Methods

Synthesis the PMN-PT Nanorods

The hydrothermal method was used to synthesis the PMN-PT nanorods. Poly(ethylene glycol)-200 (PEG200) and methanol (MeOH) mixture (PEG200/MeOH at a 1:2 volume ratio) were used as the solvent for the starting materials, and 1,1,1-tris (methylol)ethane (THOME) was used as the complexing agent. Stoichiometric amounts (corresponding to the 0.7PMN-0.3PT composition) of lead acetate trihydrate, magnesium 2,4-pentanedionante dehydrate (MgAA), niobium ethoxide, and titanium diisopropoxide bisacetyl acetonate (TIAA) were used to prepare the

* Correspondence: xzliu@uestc.edu.cn
[1]State Key Laboratory of Electronic Thin Film and Integrated Devices, School of Microelectronics and Solid-State Electronics, University of Electronic Science and Technology of China, Chengdu 610054, China
Full list of author information is available at the end of the article

Springer

Li et al. Nanoscale Research Letters (2016) 11:49

Page 2 of 4

Pb-Mg-Nb-Ti (PMNT) sol-gel. Lead acetate trihydrate, MgAA, and THOME were mixed with PEG200/MeOH mixture with strong stirring to form a Pb-Mg solution. In a separate reaction flask, niobium ethoxide, TIAA, and THOME were also mixed with PEG200/MeOH mixture with strong stirring to form an Nb-Ti solution. After stirring for 2 h at room temperature, these two solutions were then mixed together and stirred for about 4 h to form a clear yellow PMNT sol. The PMNT sol was dispersed into deionized (DI) water with strong stirring in the ratio of 1:10. Polyacrylic acid was introduced to the solution as surfactants to produce PMN-PT nanorods. Then, KOH was added into the yellow solution with quickly stirring and a white precipitate was formed. The suspension was sealed into a Teflon-lined stainless steel autoclave with the capacity of 80 ml and kept in an oven at 235 °C for 24 h. After cooling to room temperature, the suspension was washed with ethanol and DI water six times and dried at 100 °C in an oven for 6 h. Grey powder consisted of 0.7PMN-0.3PT nanorods was obtained.

Measurements

The morphology characteristics of products were determined by scanning electron microscope (SEM, Inspect F50). The structure and phase composition were investigated by powder X-ray diffractometer (XRD, DX1000) with Cu Kα of 0.1542 nm (40 kV, 30 mA) radiation. The microstructure of the PMN-PT nanorod was investigated by transmission electron microscopy (TEM, Tecnai G2 F20 S-TWIN). The piezoelectric coefficient of single PMN-PT nanorods was measured by atomic force microscopy (AFM, SEIKO SPA300HV) using a contact model.

Results and Discussion

To study the effects of different polyacrylate acid (PAA) contents on the formation of PMN-PT nanorods, the hydrothermal reaction was carried out at 235 °C for 24 h. The concentrations of PAA are 0, 0.45, 0.64, 0.82, 1.0, and 1.19 g/ml, respectively. The phases of corresponding samples were checked by XRD with Cu Kα of 0.1542 nm radiation. The XRD pattern of samples synthesized with different PAA concentrations are shown in Fig. 1. It could be indicated that the pyrochlore phases appear as the major phase with PAA concentration of 0 and 0.45 g/ml. The diffraction peaks of perovskite phase appeared, and its intensity is enhanced with the increasing of PAA concentration. It means the perovskite phase grows at the expense of the pyrochlore phase. Once the hydrothermal condition satisfied the threshold of nucleation, PMN-PT nuclei would form at the initial stage. The functional groups in PAA would tend to absorb on the surface of PMN-PT nuclei resulting in the surface energy decrease. The perovskite nuclei would be thermodynamically stable and could start to grow. An

Fig. 1 XRD pattern of PMN-PT synthesized at 235 °C with different concentration of PAA
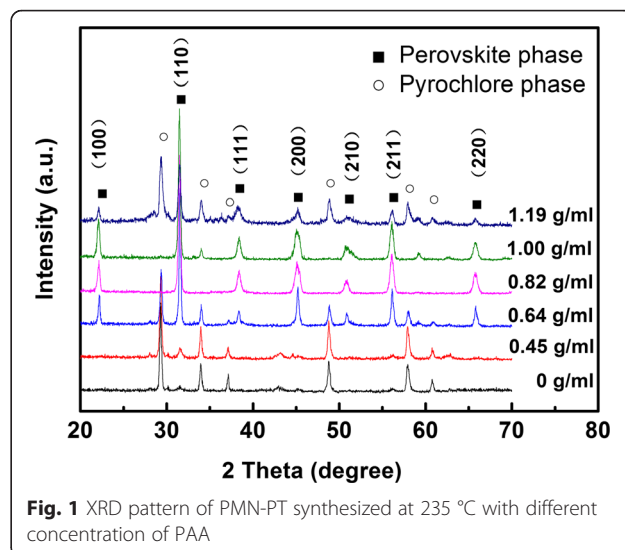
almost pure perovskite phase appears at PAA concentration of 0.82 g/ml. The diffraction peaks reveal that PMN-PT nanorods have good crystallized. However, the pyrochlore phase appears as the concentration of PAA increases above 0.82 g/ml. The amount of pyrochlore phase increases as PAA concentration increased. At high PAA concentration, the PAA attached to the PMN-PT nuclei surface in the form of a shell at the nucleation stage. The polymer shell will inhibit the crystal growth of PMN-PT nuclei.

The morphology of samples synthesized with different concentrations of PAA are shown in Fig. 2. There is almost no nanorod product but cluster of nanoflowers when the concentration of PAA is 0 and 0.45 g/ml. According to XRD results, the morphology of the pyrochlore phase is nanoflower-like. As the concentration of PAA increases from 0.45 to 0.82 g/ml, more nanorods formed and the ratio of nanoflower decreased. As we know, it needs more energy to form perovskite structure than pyrochlore. The functional groups of PAA would improve the adsorption behaviors on the PMN-PT nuclei surface. The surface energy of different crystal faces has strong influence on the growth speed. At low PAA concentration, not all the crystal growth surface contacted with PAA. The added polymers perform as capping agents that chemisorb at the side surfaces of the nanorod during the growth of PMN-PT nuclei [16]. Therefore, the length of the PMN-PT nanorod increases along [100] orientation, and the growth in the radial direction is hindered. Pure nanorod products with perovskite structure are obtained when the concentration of PAA is 0.85 g/ml. However, the amount of nanorods decreases and the length of the rod got shorter when the concentration of PAA is increasing from 0.82 to 1.19 g/ml. It could be due to the excess of PAA adsorbed on the surface of PMN-PT nuclei as a shell
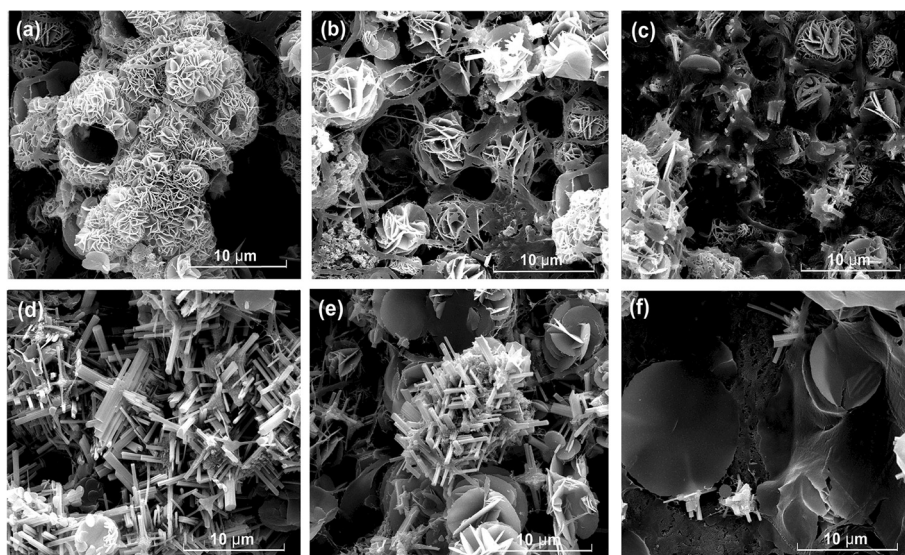
Li *et al. Nanoscale Research Letters* (2016) 11:49

Page 3 of 4

Fig. 2 SEM images of the products with PAA concentration of 0 g/ml (**a**), 0.45 g/ml (**b**), 0.64 g/ml (**c**), 0.82 g/ml (**d**), 1.0 g/ml (**e**), and 1.19 g/ml (**f**)

which hindered the crystal growth of PMN-PT nuclei at the nucleation stage. Meanwhile, the morphology of pyrochlore phase becomes nanoflake.

The morphologies, microstructures, and crystalline phases of the PMN-PT nanorods were performed by TEM and SAED (selected area electron diffraction), as shown in Fig. 3. Low-magnification TEM image of Fig. 3a shows that the nanorods have cuboid morphology and the size in radial direction is about 193 nm. The high-resolution TEM image shown in Fig. 3b further reveals that the nanorods have a good single crystal structure. Moreover, the lattice spacing of 0.402 nm corresponds to the (100) lattice plane, indicating the nanorod grow along [100] direction. The inset SAED pattern in Fig. 3b reveals that PMN-PT nanorods are structurally uniform and single crystal.

The PMN-PT nanorods were dispersed by ethanol. Then, a drop of suspension was put on Au/Ti-covered silicon wafer and dried in air. The d_{33} coefficient of single PMN-PT nanowire was measured by AFM using a contact model. The relationship of piezoelectric displacement and voltage applied on AFM tip was plotted in Fig. 4, with 3D AFM image inserted. The equation for the fitted curve (red line) is displacement = −0.01895 + 0.409 × voltage, which means the piezoelectric coefficient d_{33} determined from the slope of the linear fitting is 409 pm/V. This value is slightly larger than d_{33} value of 0.72PMN-0.28PT nanorod (381 pm/V) [15]. It is worth noting that the d_{33} value of PMN-PT nanorod is much lower than the PMN-PT ceramics. This is due to the fact that the PMN-PT nanorod is not been polarized. The ferroelectric domains of the nanorod, as we can see in Fig. 3a, have different spontaneous polarization directions. Moreover, the d_{33} value of PMN-PT nanorod is measured along [010] or [001] direction, but the d_{33} value of textured PMN-PT ceramics is measured along [111] direction.
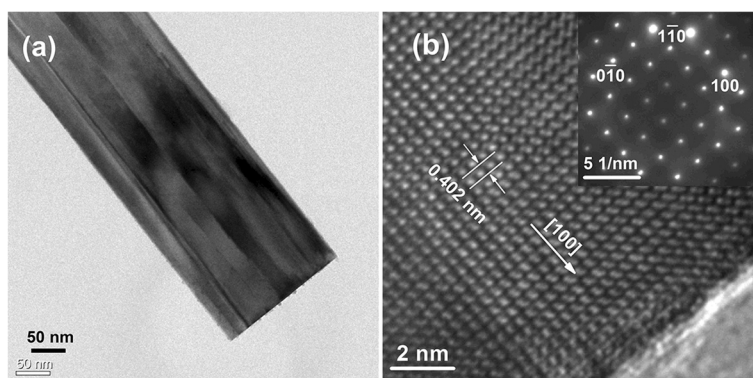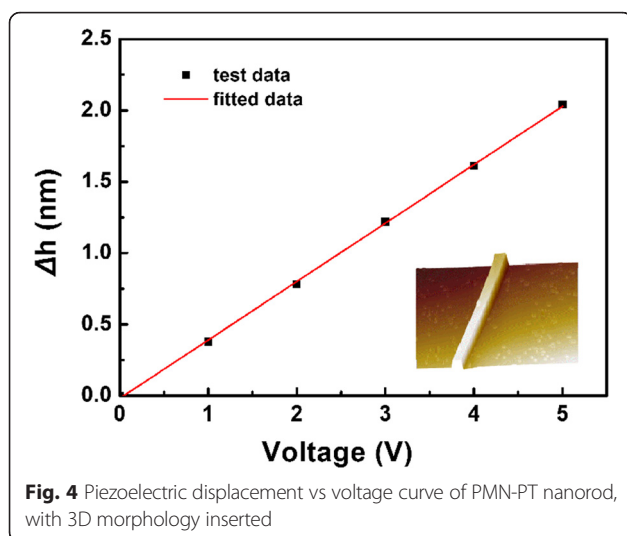

Fig. 3 a Low-magnification TEM image of PMN-PT nanorod. **b** High-angle annular dark-field (HAADF) image of a nanorod and the insert is electron diffraction pattern

Li *et al. Nanoscale Research Letters* (2016) 11:49

Page 4 of 4

Fig. 4 Piezoelectric displacement vs voltage curve of PMN-PT nanorod, with 3D morphology inserted

Conclusions

Single crystalline PMN-PT nanorods of cuboid morphology were obtained at 235 °C with the addition of PAA in hydrothermal reaction. As PAA concentration increased from 0.45 to 0.82 g/ml, the length of the PMN-PT nanorod increased while the growth in the radial direction was hindered. An almost pure perovskite phase (PMN-PT nanorod) appeared at a PAA concentration of 0.82 g/ml. The orientation growth of PMN-PT was attributed to the surface energy difference caused by absorption of PAA on different crystal plane. The piezoelectric coefficient of 0.7PMN-0.3PT nanorod was 409 pm/V, which provides a great potential application in manufacturing piezoelectric nanodevices.

Abbreviations

AFM: atomic force microscopy; DI: deionized; HAADF: high-angle annular dark-field; LED: light-emitting diode; MeOH: methanol; MgAA: magnesium 2,4-pentanedionante dehydrate; PAA: polyacrylate acid; PEG200: poly(ethylene glycol)-200; PMN-PT: $(1-x)Pb(Mg_{1/3}Nb_{2/3})O_3-xPbTiO_3$; PMNT: Pb-Mg-Nb-Ti; PZNT: $(1-x)PbZn_{1/3}Nb_{2/3}O_3-xPbTiO_3$; PZT: Pb-based lanthanum-doped zirconate titanates; SAED: selected area electron diffraction; SEM: scanning electron microscope; TEM: transmission electron microscopy; THOME: 1,1,1-tris (methylol)ethane; TIAA: titanium diisopropoxide bisacetyl acetonate; XRD: X-ray diffractometer.

Competing Interests

The authors declare that they have no competing interests.

Authors' Contributions

CL gave the final approval of the version to be published and measured and analyzed the experimental date. XL directed the project. WL and DX were involved in the discussion of the manuscript. CL and KH performed the experiments. All authors read and approved the final manuscript.

Author details

[1]State Key Laboratory of Electronic Thin Film and Integrated Devices, School of Microelectronics and Solid-State Electronics, University of Electronic Science and Technology of China, Chengdu 610054, China. [2]School of Material Science and Engineering, Jiangsu University, Zhenjiang 212013, China.

References

1. Noheda B, Cox DE, Shirane G, Park SE, Cross LE, Zhong Z (2001) Polarization rotation via a monoclinic phase in the piezoelectric 92% $PbZn_{1/3}Nb_{2/3}O_3$-8% $PbTiO_3$. Phys Rev Lett 86:3891–3894
2. Xu S, Hansen BJ, Wang ZL (2010) Piezoelectric-nanowire-enabled power source for driving wireless microelectronics. Nat Commun 1:93
3. Wang ZY, Hu J, Suryavanshi AP, Yum K, Yu MF (2007) Voltage generation from individual $BaTiO_3$ nanowires under periodic tensile mechanical load. Nano Lett 7:2966–2969
4. Hwang GT, Yang J, Yang SH, Lee HY, Lee M, Park DY, Han JH, Lee SJ, Jeong CK, Kim J, Park KI, Lee KJ (2015) A reconfigurable rectified flexible energy farvester via solid-state single crystal grown PMN-PZT. Adv Energy Mater 5: 1500051
5. Zhang Y, Zhang YJ, Xue XY, Cui CX, He B, Nie YX, Deng P, Wang ZL (2014) PVDF-PZT nanocomposite film based self-charging power cell. Nanotechnology 25:105401
6. Mao YC, Zhao P, McConohy G, Yang H, Tong YX, Wang XD (2014) Sponge-like piezoelectric polymer films for scalable and integratable nanogenerators and self-Powered electronic systems. Adv Energy Mater 4:1301624
7. Gao T, Liao JJ, Wang JS, Qiu YQ, Yang Q, Zhang M, Zhao Y, Qin LF, Xue H, Xiong ZX, Chen LF, Wang QM (2015) Highly oriented $BaTiO_3$ film self-assembled using an interfacial strategy and its application as a flexible piezoelectric generator for wind energy harvesting. J Mater Chem A 3:9965–9971
8. Bhatia B, Damodaran AR, Cho HN, Martin LW, King WP (2014) High-frequency thermal-electrical cycles for pyroelectric energy conversion. J Appl Phys 116:194509
9. Wang XD, Song JH, Liu J, Wang ZL (2007) Direct-current nanogenerator driven by ultrasonic waves. Science 316:102–105
10. Hu YF, Zhang Y, Xu C, Zhu GA, Wang ZL (2010) High-output nanogenerator by rational unipolar assembly of conical nanowires and its application for driving a small liquid crystal display. Nano Lett 10:5025–5031
11. Kusumoto K, Sekiya T (1998) Processing and properties of $(1-x)Pb(Mg_{1/3}Nb_{2/3})O_3 \cdot xPbTiO_3$ solid solutions from PbO- and MgO-excess compositions. Mater Res Bull 33:1367–1375
12. Sabolsky EM, James AR, Kwon S, Trolier-McKinstry S, Messing GL (2001) Piezoelectric properties of <001> textured $Pb(Mg_{1/3}Nb_{2/3})O_3$-$PbTiO_3$ ceramics. Appl Phys Lett 78:2551–2553
13. Sun CL, Qin LF, Li F, Wang QM (2009) Piezoelectric energy harvesting using single crystal $Pb(Mg_{1/3}Nb_{2/3})O_3$-$xPbTiO_3$ (PMN-PT) device. J Intell Mater Syst Struct 20:559–568
14. Sun CL, Shi JA, Wang XD (2010) Fundamental study of mechanical energy harvesting using piezoelectric nanostructures. J Appl Phys 108:034309
15. Xu SY, Poirier G, Yao N (2012) PMN-PT nanowires with a very high piezoelectric constant. Nano Lett 12:2238–2242
16. Xu G, Ren ZH, Du PY, Weng WJ, Shen G, Han GR (2005) Polymer-assisted hydrothermal synthesis of single-crystalline tetragonal perovskite $PbZr_{0.52}Ti_{0.48}O_3$ nanowires. Adv Mater 17:907–910